Topical Treatment of Human Skin and Cultured Keratinocytes with High-Dose Spironolactone Reduces XPB Expression and Induces Toxicity

M. Alexandra Carpenter[1] and Michael G. Kemp[1]

Spironolactone (SP) is used to treat a variety of disparate disease states ranging from heart failure to acne through antagonism of the mineralocorticoid and androgen receptors. Although normally taken as an oral medication, recent studies have explored the topical application of SP onto the skin. However, because SP induces the proteolytic degradation of the XPB protein, which plays critical roles in DNA repair and transcription, there may be safety concerns with the use of topical SP. In this study, we show that the topical application of a high concentration of either SP or its metabolite canrenone onto human skin ex vivo lowers XPB protein levels and induces toxic responses in the epidermis. Interestingly, although SP and canrenone both inhibit cell proliferation, induce replication stress responses, and stimulate apoptotic signaling at high concentrations in cultured keratinocytes in vitro, these effects were not correlated with XPB protein loss. Thus, high concentrations of SP and canrenone likely inhibit cell proliferation and induce toxicity through additional mechanisms to XPB proteolytic degradation. This work suggests that care may need to be taken when using high concentrations of SP directly on human skin.

JID Innovations (2021);**1:**100023 doi:10.1016/j.xjidi.2021.100023

INTRODUCTION

First recognized for its ability to reduce arterial pressure in patients with hypertension by increasing the excretion of sodium and water, the mineralocorticoid receptor (MR) antagonist spironolactone (SP) was an early drug used for improving blood pressure and treating heart failure (Cranston and Juel-Jensen, 1962; Kagawa et al., 1957; Liddle, 1957; Sturtevant, 1958). It has also been employed in treating ascites due to cirrhosis (Moore and Aithal, 2006) and diabetic kidney disease (Dojki and Bakris, 2017). SP was later found to also antagonize androgen receptors (Bonne and Raynaud, 1974; Corvol et al., 1975), which led to its use for androgen-associated skin maladies such as acne and hair growth dysfunction (Rathnayake and Sinclair, 2010; Sinclair et al., 2011). Besides having feminizing effects in males (Bowman et al., 2012) and sometimes leading to hyperkalemia (Park and Skopit, 2016), SP is generally considered to be a safe medication.

Interestingly, several recent in vitro, cell-based drug repurposing screens have identified SP as a compound with diverse functions ranging from promoting antitumor immunity (Leung et al., 2013) to inhibiting DNA repair (Alekseev et al., 2014; Shahar et al., 2014) and viral transcription (Verma et al., 2016). Alekseev et al. (2014) linked the effect on DNA repair to the XPB protein, a DNA translocase that plays important roles in the removal of UV photoproducts from DNA and in the initiation of transcription (Compe and Egly, 2012; Fishburn et al., 2015; Fuss and Tainer, 2011). Mutations in XPB lead to the skin cancer–prone disease xeroderma pigmentosum and a progeroid and neurodegenerative disease known as Cockayne syndrome. Complete loss of the protein in mice is embryonic lethal (Andressoo et al., 2009).

SP was found to induce the rapid proteolytic degradation of XPB by ubiquitination and proteasomal degradation (Alekseev et al., 2014). Recent studies have indicated a role for CDK7, the E3 ubiquitin ligase SCF^{FBXL18} (Ueda et al., 2019), and the ubiquitin-selective segregase VCP/p97 (Chauhan et al., 2021) in this process. SP-mediated loss of XPB has been reported to occur in a variety of cell types in vitro (Alekseev et al., 2014; Elinoff et al., 2018; Kemp et al., 2019; Lacombe et al., 2016; Martella et al., 2020; Szalat et al., 2018), in human skin explants ex vivo (Choi et al., 2020; Kemp et al., 2019), and in rat lungs in vivo (Elinoff et al., 2018). The consequences of SP treatment on XPB protein stability, DNA repair, and transcription have all appeared to be specific to SP and not specific to either its metabolites or the related MR antagonist eplerenone (Gabbard et al., 2020).

Although SP has traditionally been used as an oral medication, there has been an interest in developing alternative formulations (Abdel-Raouf et al., 2021; Biyashev et al., 2020; Ilic et al., 2021; Kelidari et al., 2017, 2016, 2015; Salama et al., 2019) that can be applied topically on the skin for beneficial purposes and to avoid the systemic effects that usually limit its use to females (Bowman et al., 2012). In

[1]*Department of Pharmacology and Toxicology, Boonshoft School of Medicine, Wright State University, Dayton, Ohio, USA*

Correspondence: Michael G. Kemp, Department of Pharmacology and Toxicology, Boonshoft School of Medicine, Wright State University, Dayton, Ohio 45435, USA. E-mail: mike.kemp@wright.edu

Abbreviations: Can, canrenone; KC, keratinocyte; MR, mineralocorticoid receptor; PCNA, proliferating cell nuclear antigen; SP, spironolactone

Received 30 December 2020; revised 15 April 2021; accepted 19 April 2021; accepted manuscript published online 6 May 2021; corrected proof published online 30 August 2021

Cite this article as: JID Innovations 2021;1:100023

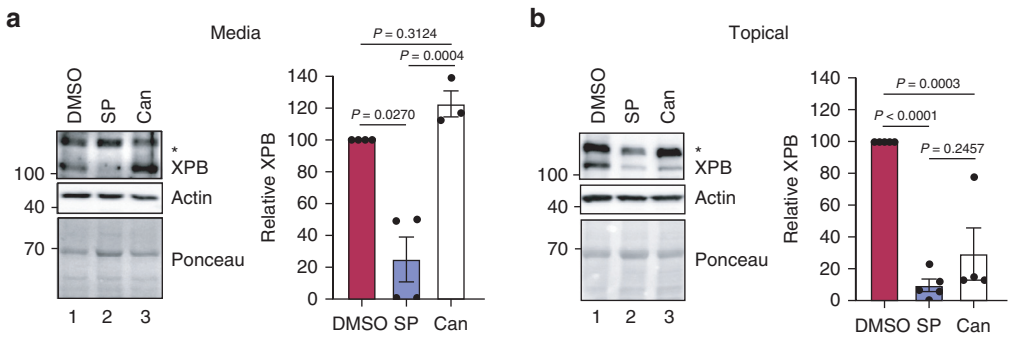

Figure 1. Topical treatment of human skin with SP and Can depletes the epidermis of the XPB protein. (**a**) Human skin biopsies placed in hanging well inserts in a cell culture dish were treated twice over 2 days with either 20 μM SP, Can, or vehicle (DMSO) added to the cell culture medium below the biopsy. Immunoblotting was performed with total epidermal protein, and the relative level of XPB protein was calculated from three to four different skin donors. (**b**) Human skin from four to five different donors was treated and processed as in **a** except that 25 μl of 120 mM SP or Can was added to the top of the skin biopsy. The asterisk (*) above the XPB band denotes a nonspecific band recognized by the anti-XPB antibody. One-way ANOVA was used to determine the statistical significance. Can, canrenone; SP, spironolactone.

addition, because glucocorticoids can induce skin atrophy and inhibit wound healing owing to aberrant stimulation of MRs, SP and related MR antagonists have been employed in experimental studies in mouse models and human subjects to counteract some of the negative effects of glucocorticoids (Boix et al., 2018; Maubec et al., 2015; Nguyen et al., 2016). These topical preparations have involved the use of a 5% SP (120 mM) gel, which is a considerably higher concentration than the peak blood concentration of 190 nM typically found after a standard oral dose of 100 mg SP (Gardiner et al., 1989).

To address the potential effects that topical high-dose SP administration may have on XPB protein levels and genomic stress responses in the skin, we examined the effect of treating human skin with a high concentration of SP or its major metabolite canrenone (Can) (Gardiner et al., 1989). We found that both SP and Can induced a loss of XPB protein, altered the expression of protein markers of proliferation and DNA damage, and induced epidermal toxicity in human skin ex vivo. Using cultured keratinocytes (KCs) in vitro, we found that both SP and Can induced replication stress and apoptosis but that these responses are not correlated with a loss of XPB protein. Coupled with previous research showing that SP-mediated loss of XPB negatively influences responses to UVR in the skin (Choi et al., 2020; Kemp et al., 2019), these results indicate that high concentrations of SP and Can induce toxicity in epidermal skin cells through an XPB-independent mechanism.

RESULTS

Epidermal XPB protein levels are reduced by topical treatment with SP

As we have previously reported (Choi et al., 2020; Kemp et al., 2019), the addition of 20 μM SP (10 nmol) twice over 2 days to cell culture medium maintained below small, 8 mm human skin explants reduced epidermal XPB protein expression by 50 to >95%, depending on the individual skin sample (Figure 1a). In contrast, the addition of 20 μM SP topically on the skin did not affect XPB protein levels (data not shown). Studies with mouse and human skin have used a much higher concentration of SP (5% or 120 mM) that is delivered in a smaller volume when treating the skin topically (Boix et al., 2018; Maubec et al., 2015; Nguyen et al., 2016). Therefore, we also examined the effect of adding 25 μl of 120 mM SP (3 μmol; prepared in 100% DMSO) to the top of 8 mm diameter skin explants on 2 consecutive days. As shown in Figure 1b, SP induced a loss of XPB protein to a similar extent as 20 μM SP added to the culture medium below the skin explant. Quantitation from five independent skin samples revealed that the topical SP reduced XPB protein expression by 77−100% (Figure 1b).

Can is a metabolite of SP that has been reported to have similar effects of SP in counteracting glucocorticoid effects on epidermal thinning and wound healing (Maubec et al., 2015) but is not reported to deplete XPB in cultured cells (Kemp et al., 2019; Ueda et al., 2019). Interestingly, topical addition of 120 mM Can also depleted epidermal XPB protein by nearly 90% in three of the four skin samples that were tested (Figure 1b). In contrast, when Can was added to the medium below the skin explant at a concentration of 20 μM, it did not reduce XPB protein levels (Figure 1a), as predicted by the studies with cultured cells in vitro. The difference in XPB depletion with differing concentrations of Can prompted us to further investigate the dose dependencies of SP and Can in cultured KCs in vitro.

SP is much more effective than Can at reducing XPB protein expression in KCs in vitro

Owing to the unexpected effect of topical, high-dose Can in depleting epidermal XPB protein levels in the skin ex vivo (Figure 1b), we next investigated the relationship between XPB levels and SP or Can concentrations in vitro. HaCaT KCs were treated with SP or Can at concentrations ranging from 1 μM to 1 mM for 6 hours. As shown in Figure 2a, 10 μM SP

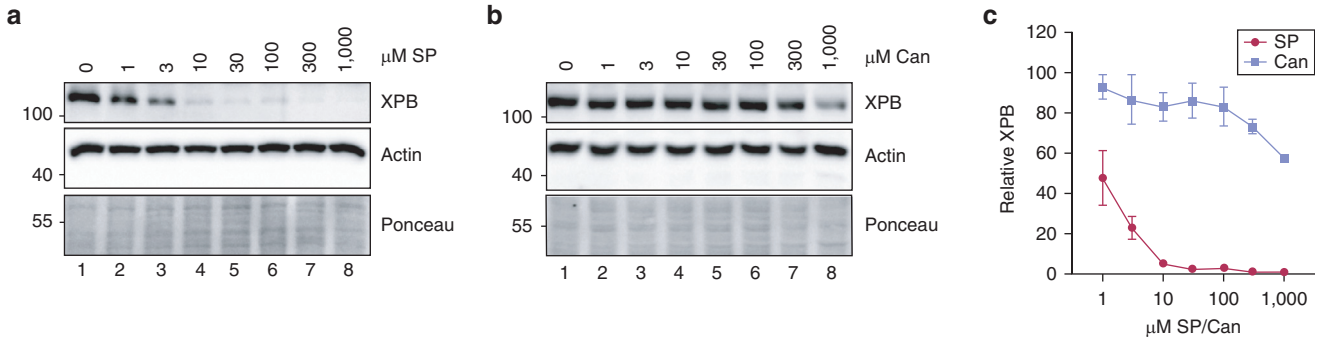

Figure 2. SP and Can have different effects of XPB protein depletion on keratinocytes in vitro. (**a**) HaCaT keratinocytes were treated for 6 hours with the indicated concentrations of SP. Cell lysates were then analyzed by immunoblotting. (**b**) Cells were treated with increasing concentrations of Can as in (**a**). (**c**) XPB protein levels from three independent experiments performed as in (**a**) and (**b**) were quantified and graphed. Two-way ANOVA revealed that whereas all concentrations of SP induced a significant decrease in XPB protein levels in comparison with those of the untreated control ($P < 0.0001$), only the two highest concentrations of Can were associated with a decrease in XPB protein ($P < 0.01$). Can, canrenone; SP, spironolactone.

potently reduced XPB protein levels by >95%, and even doses as low as 1 μM significantly reduced XPB protein by approximately 50%. In contrast, XPB protein levels were largely resistant to the effects of Can except at the highest 300 μM and 1 mM concentrations (Figure 2b). The effect of SP and Can on XPB protein levels were then quantified and graphed from three independent experiments (Figure 2c), which confirmed the significant differences between SP and Can in reducing XPB protein levels.

High concentrations of SP and Can negatively affect cell proliferation in vitro

Preliminary experiments indicated that treatment of HaCaT cells with high concentrations of SP and Can also negatively affect cell proliferation. We therefore next performed cell proliferation assays in HaCaT KCs treated with increasing concentrations of SP and Can for 48 hours. As shown in Figure 3a, although SP was more potent than Can, both drugs negatively affected cell viability when cells were treated with concentrations ≥100 μM. These effects were not simply due to the high concentrations of DMSO used in the treatments (up to 0.83%; Figure 3b). Similar results were observed in telomerase-immortalized, neonatal foreskin KCs (Figure 3c). Interestingly, the related MR antagonist eplerenone did not negatively affect cell proliferation (Figure 3d), which suggests that this inhibition of proliferation is specific to SP and Can.

Analysis of XPB protein depletion and cell survival by nonlinear regression showed no clear correlation between the effect of SP and Can on XPB protein expression and cell viability (Table 1). For example, whereas 1 μM SP was sufficient to reduce XPB protein expression in HaCaT cells by 50%, >50-fold more SP (67 μM) was required to inhibit cell proliferation by 50%. Moreover, Can was 1,000-fold less effective at reducing XPB protein levels but only three-fold less inhibitory than SP on cell proliferation. Although somewhat more sensitive to SP and Can, similar effects were seen in telomerase-immortalized neonatal KCs (Table 1). Thus, we conclude that the effects of high concentrations of SP and Can on XPB protein expression do not fully account for the effect of these compounds on cell proliferation and survival.

High concentrations of SP and Can induce replication stress and apoptosis in KCs in vitro

To further examine the mechanism by which high concentrations of SP and Can inhibit KC proliferation, we analyzed canonical markers of DNA damage and replication stress by immunoblotting. As shown in Figure 4a, treatment of HaCaT cells with 1 mM SP led to robust phosphorylation of the checkpoint signaling protein Chk1 (Dai and Grant, 2010) within a few hours of SP administration and led to mono-ubiquitination of the replicative polymerase clamp protein proliferating cell nuclear antigen (PCNA), which is involved in signaling the recruitment of specialized translesion synthesis polymerases to DNA (Kanao and Masutani, 2017). At later time points, phosphorylation of the heterochromatin protein KAP1 and histone variant H2AX were also observed (Figure 4b). Interestingly, phosphorylation of the tumor suppressor protein p53 and the checkpoint kinase Chk2, two additional common biomarkers of the DNA damage response, was not observed (Figure 4a). Dose–response experiments revealed that SP-induced Chk1 phosphorylation was only observed at high concentrations of SP above those required to deplete XPB protein (Figure 4c). Can also induced the phosphorylation of Chk1 but not of Chk2 (Figure 4d) in a manner dependent on ATR kinase activity (Figure 4e). ATR–Chk1 signaling is known to be activated by perturbations in DNA replication (Saldivar et al., 2017), and BrdU (Sigma-Aldrich) pulse labeling of genomic DNA showed that treatment of HaCaT cells with either 1 mM SP or Can resulted in a rapid inhibition of DNA synthesis within 15 minutes of treatment (Figure 4f). Together, these results indicate that high concentrations of SP and Can induce replication stress in a manner that is not directly correlated with changes in XPB protein levels.

To follow up on our data showing that SP induces KAP1 and H2AX phosphorylation at late time points after treatment (Figure 4a and b), we treated SP and Can with increasing concentrations of SP or Can for 12 hours. These phosphorylation events were only observed after treatment with SP and Can concentrations ≥300 μM (Figure 4g). Cleavage of caspase 3 and the caspase substrate PARP was found to be correlated with these phosphorylation events in both time-course and dose-response experiments (Figure 4a, b, and

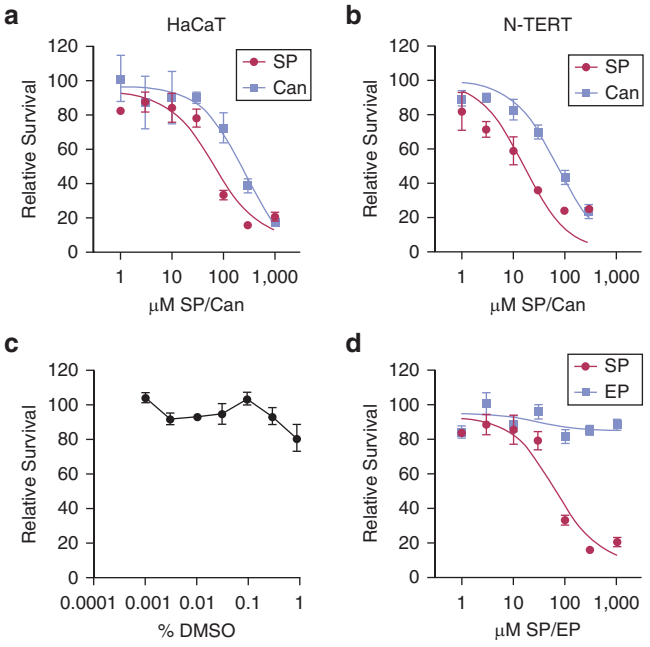

Figure 3. High concentrations of SP and Can inhibit cell proliferation in keratinocytes in vitro. (**a**) HaCaT keratinocytes were treated with increasing concentrations of SP or Can. MTT assays were performed 2 days later. The relative absorbance values were normalized to values for the vehicle (DMSO)-treated cells, and the relative survival was then graphed from three to five independent experiments. IC_{50} values for each individual experiment were determined by nonlinear regression. The *t*-tests revealed significant differences between the IC_{50} values for SP and Can ($P = 0.017$). (**b**) HaCaT cells were treated with the indicated concentrations of DMSO for 2 days. MTT assays were performed to monitor cell proliferation and/or survival. Results are the average (and SEM) from five independent experiments. One-way ANOVA showed no significant difference in relative survival. (**c**) N-TERTs were analyzed as in **(a)**, and the results from two experiments were graphed. (**d**) HaCaT keratinocytes were treated with increasing concentrations of SP or EP. MTT assays were performed 2 days later. The relative absorbance values were normalized to values for the vehicle (DMSO)-treated cells, and the relative survival was then graphed from three to five independent experiments. Can, canrenone; EP, eplerenone; IC_{50}, half-maximal inhibitory concentration; MTT, 3-(4,5-dimethylthiazol-2-yl)-2,5-diphenyl tetrazolium bromide; N-TERT, telomerase-immortalized neonatal keratinocyte; SP, spironolactone.

g). Although replication stress could lead to DNA double-strand break formation and to the phosphorylation of ATM substrates (including Chk2, H2AX, and KAP1) (Goodarzi et al., 2008; Kitagawa and Kastan, 2005), the absence of Chk2 phosphorylation in SP- and/or Can-treated cells coupled with the delayed induction of H2AX and KAP1 phosphorylation suggested an alternative mechanism for the phosphorylation of these latter substrates. Indeed, there have been reports that H2AX phosphorylation can be induced in cells undergoing apoptosis (Mukherjee et al., 2006; Solier and Pommier, 2009). To determine whether the H2AX phosphorylation we observed in cells treated with SP and Can was dependent on apoptotic signaling, we treated HaCaT cells with the pan-caspase inhibitor Z-VAD-FMK and then exposed the cells to a high concentration of SP or Can. As shown in Figure 4h, the caspase inhibitor nearly completely blocked H2AX induction by SP and Can (Figure 4i). Thus, we conclude from these results that high doses of SP and Can

Table 1. Analysis of Concentrations of SP and Can Required to Reduce XPB Protein Expression and Cell Proliferation

	HaCaT		N-TERT	
	XPB	Survival	XPB	Survival
SP	0.97 ± 0.35 μM	64 ± 12 μM	1.59 ± 0.36 μM	16 ± 5 μM
Can	1,044 ± 226 μM	211 ± 26 μM	n.d.	75 ± 15 μM

Abbreviations: Can, canrenone; n.d., not determined; N-TERT, telomerase-immortalized neonatal keratinocyte; SP, spironolactone.

Nonlinear regression was used to calculate the concentration of SP and Can required to deplete XPB protein and inhibit proliferation by 50% from the data generated in Figures 2 and 3. The average (and SEM) are shown from two to five independent experiments.

necessary to inhibit cell proliferation (Figure 3) are correlated with increased replication stress and apoptotic signaling but not effects on XPB protein levels (Figure 4).

Treatment with high concentrations of SP and Can induces toxicity in skin ex vivo

We next revisited our studies examining the effects of applying high concentrations of SP and Can topically on human skin to extend our findings with KCs in vitro. We therefore probed epidermal lysates from the human skin samples treated in Figure 1 for PCNA and phosphorylated histone H2AX. As shown in Figure 5a–c and Table 2, both SP- and Can-treated skin displayed an approximately three-fold increase in H2AX phosphorylation and a significant reduction in the levels of the cell proliferation marker protein PCNA. Supplementation of skin explant media with 20 μM SP or Can did not induce this response (Figure 5d), which further supports our in vitro findings that the induction of H2AX phosphorylation by SP and/or Can is not correlated with effects on XPB protein levels.

Consistent with data showing that SP and Can induced caspase signaling in HaCaT cells in vitro (Figure 4a, g, and h), we observed increased PARP cleavage in human skin explants treated topically with 120 mM SP or Can (Figure 5e). Furthermore, H&E staining revealed a striking separation of the epidermis from the dermis in SP- and/or Can-treated skin (Figure 5f), suggesting evidence of extensive toxicity caused by SP and Can. Thus, we conclude that similar to KCs in vitro, human skin is susceptible to toxic effects of high concentrations of SP and its metabolite Can.

DISCUSSION

SP is used to treat a variety of human disorders but has not been found to induce any increased risk of cancer or general toxicity (Biggar et al., 2013; Mackenzie et al., 2017), which might otherwise be expected if the compound were to lead to a significant loss of XPB, an essential regulator of nucleotide excision repair and transcription (Compe and Egly, 2012). However, we have observed in this study that treatment of human skin ex vivo and KCs in vitro with a high concentration of the drug does have some negative consequences, including the depletion of XPB protein, an inhibition of cell proliferation, and induction of replication stress and apoptotic signaling responses. It should be noted that previous mouse and human studies employing a similarly high

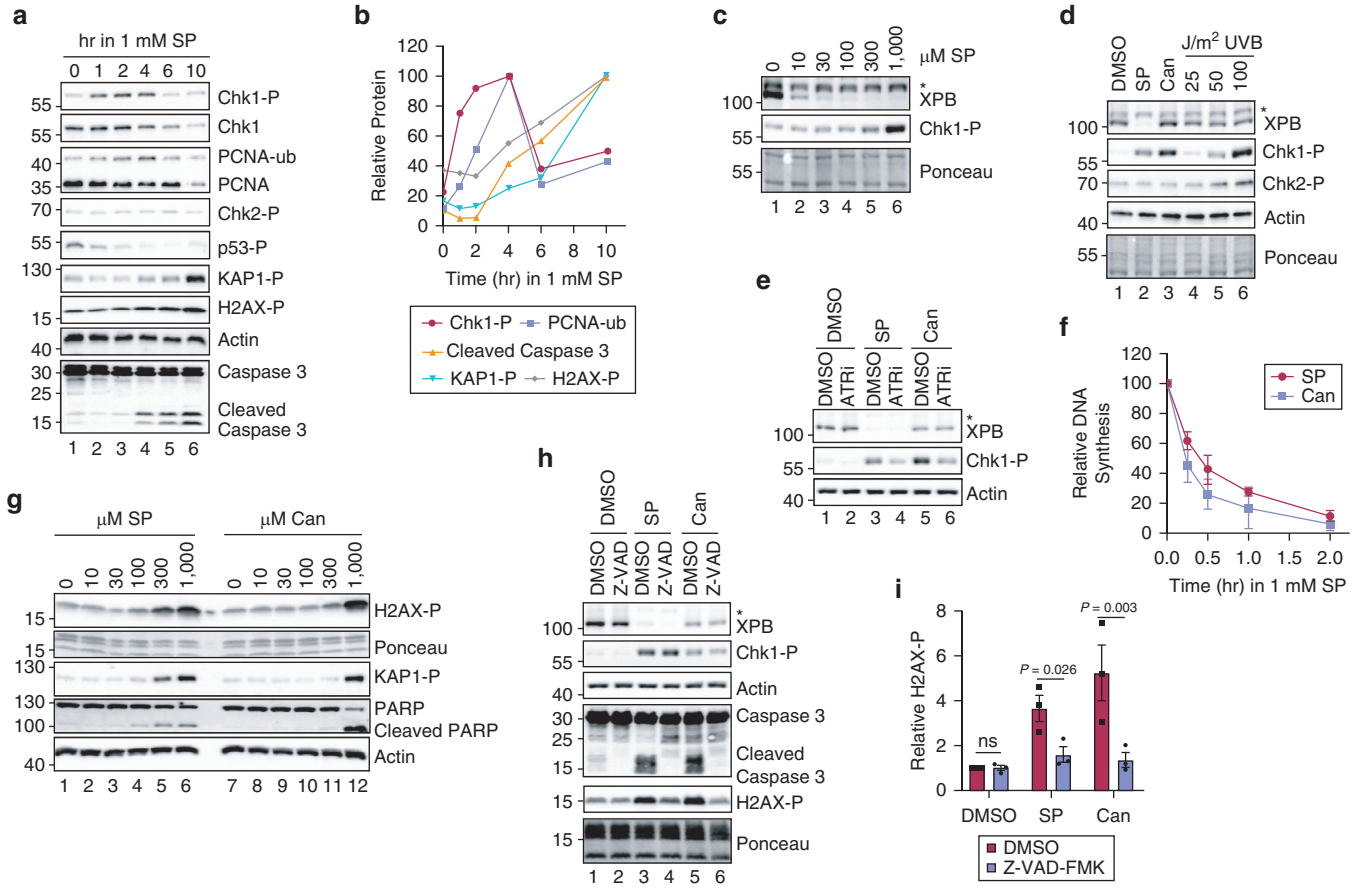

Figure 4. High concentrations of SP and Can induce replication stress responses and apoptosis in keratinocytes in vitro. (**a**) HaCaT keratinocytes were treated with 1 mM SP for the indicated periods of time. Immunoblotting was performed with cell lysates with antibodies targeting the indicated proteins or -P proteins. (**b**) Quantitation of protein levels in which signals were normalized to the time point at which the signal was highest. The asterisk (*) above the XPB band denotes a nonspecific band recognized by the anti-XPB antibody. (**c**) HaCaT cells were treated with the indicated concentrations of SP for 2 hours and were then analyzed by immunoblotting. (**d**) HaCaT cells were treated with vehicle (0.83% DMSO), 1 mM SP, 1 mM or Can or exposed to the indicated fluences of UVB radiation. Cell lysates were prepared 2 hours later and examined by immunoblotting. (**e**) Cells were pretreated with DMSO (0.1% DMSO) or 10 µM of the ATRi VE-821 for 30 minutes before exposure to DMSO or 1 mM SP and/or Can. Cells were harvested 2 hours later. (**f**) Cells were treated with 1 mM SP and/or Can for the indicated periods of time in which BrdU (10 µg/ml) was added to the media during the final 15 minutes before harvesting. Genomic DNA was purified and analyzed by immunoblotting with an anti-BrdU antibody. Signals were normalized to cells that were not treated with SP or Can, and the average (and SEM) relative DNA synthesis from two independent experiments was graphed. (**g**) Cells were treated for 12 hours with the indicated concentrations of SP or Can. (**h**) Cells were pretreated with DMSO (0.2% DMSO) or 20 µM of the pan-caspase inhibitor Z-VAD-FMK along with vehicle or 1 mM SP and/or Can. Cells were harvested 9 hours later. (**i**) Quantitation of H2AX phosphorylation from three independent experiments performed as in (**g**). The individual experimental values are indicated by the black squares and circles. Paired *t*-tests were used to compare the relative changes in H2AX phosphorylation. For all other experiments, the results are representative of at least two independent experiments. ATRi, ATR inhibitor; Can, canrenone; hr, hour; -P, phosphorylated; PCNA, proliferating cell nuclear antigen; SP, spironolactone; -ub, ubiquitin.

concentration of SP or Can did not report any negative effects of the drug on the skin (Boix et al., 2018; Maubec et al., 2015; Nguyen et al., 2016). Moreover, HPLC analysis showed that SP poorly penetrated through human skin placed in a Franz cell chamber (Maubec et al., 2015). We suggest that the differences in apparent toxicity in our experiments versus those in previous reports (Maubec et al., 2015; Nguyen et al., 2016) may be due to the vehicles used to apply the drug on the skin. Although the DMSO we used in our studies may be a convenient vehicle for promoting drug transit across the stratum corneum, it is not a clinically relevant vehicle for applying compounds on human skin. Thus, the concentrations of SP and Can reaching viable epidermal cells in previous studies in which the drugs were applied topically were presumably low and safe enough to avoid negative consequences. Our results shown in this study may therefore be somewhat artificial owing to the vehicle employed in our work. Nonetheless, because research is underway at improving the delivery of SP into the skin (Abdel-Raouf et al., 2021; Biyashev et al., 2020; Ilic et al., 2021; Kelidari et al., 2017, 2016, 2015; Salama et al., 2019), we suggest that care may need to be taken to ensure that such approaches do not induce toxicity or cause a reduction in XPB protein expression, which could interfere with UV photoproduct removal and increase the risk of skin carcinogenesis.

The mechanism by which high, toxic concentrations of Can affect XPB protein levels in the skin epidermis ex vivo and KCs in vitro also remains to be clarified. It is possible that the Can-induced loss of XPB occurs secondarily to cell death processes. Although caspase inhibition did not rescue Can-induced XPB protein loss (Figure 4h), there may be other cell death pathways that are taking place and that could be responsible for the unexpected XPB protein loss that we

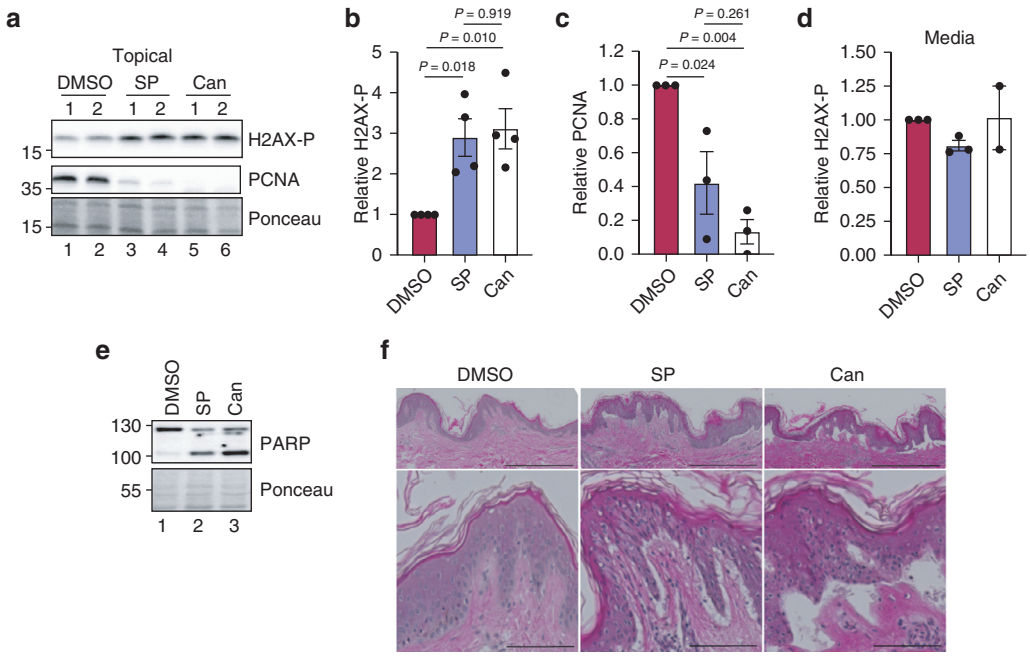

Figure 5. Treatment of human skin with high concentrations of SP and Can induces toxicity ex vivo. (**a**) Human skin explants were treated topically with DMSO, SP, or Can as in Figure 1. Epidermal lysates were probed for H2AX-P (Ser139) and PCNA. Results from replicate biopsies from a representative experiment are shown. (**b**) The relative level of H2AX-P was quantified from four independent skin samples and then graphed. One-way ANOVA was used to compare the responses between the treatment groups. (**c**) The relative level of PCNA protein was analyzed as in (**b**). (**d**) Effect of adding SP or Can to media below skin punch biopsies on basal H2AX phosphorylation. The black circles refer the individual experimental values. (**e**) Epidermal lysates from (**a**) were analyzed for PARP cleavage as a measure of apoptotic signaling. (**f**) H&E staining was performed with human skin biopsies treated as in (**a**) and viewed by microscopy at both ×4 magnification (top; bar = 0.5 mm) and ×20 magnification (bottom; bar = 0.1 mm). Note the separation of the epidermis from the dermis. Can, canrenone; H2AX-P, phosphorylated histone H2AX; PCNA, proliferating cell nuclear antigen; SP, spironolactone.

observed in both human skin ex vivo and KCs in vitro. Although Ueda et al. (2019) previously reported that a high concentration (200 μM) of a chemically reduced form of SP (SP′-OH or 7α-acetylsulfanyl-3β-hydroxy-17α-pregn-4-ene-21,17-carbolactone) was capable of causing a reduction in XPB protein levels (Ueda et al., 2019), it was not reported whether this affected cell proliferation or exhibited toxicity.

Furthermore, the mechanism by which SP and Can induce replication stress responses and apoptosis in KCs (Figure 4) and skin (Figure 5) remains to be better defined. Given that the toxic effects of high concentrations of SP and Can are not correlated with effects on XPB, we suggest that these compounds act on additional targets in cultured KCs and human skin. Consistent with a previous report that SP induces apoptosis in an MR-independent manner in human blood mononuclear cells (Sønder et al., 2006), we observed that the specific MR inhibitor eplerenone did not affect cell proliferation even at very high concentrations (Figure 3d). SP is known to target androgen and other steroid hormone receptors (Arai et al., 2015) and to inhibit various potassium channels (Caballero et al., 2003; Gómez et al., 2005), and thus, it is possible that high concentrations of SP and Can overwhelm these other receptors and transporters and rapidly alter cell physiology and ultimately cell fate. However, there may also be other unknown mechanisms by which these compounds act to induce toxic responses. The rapid inhibition of DNA synthesis (Figure 4f) and induction of replication stress responses (Figure 4a–e) indicate that these compounds

Table 2. Summary of Relative XPB Protein, H2AX Phosphorylation, and PCNA Protein Levels in Skin Biopsies Ex Vivo

	Relative XPB Protein						Relative H2AX Phosphorylation						Relative PCNA		
	Topical			Media			Topical			Media			Topical		
Skin Sample Number	DMSO	SP	Can	DMSO	SP	Can	DMSO	SP	Can	DMSO	SP	Can	DMSO	SP	Can
1	100	23	—	100	50	—	1.0	1.9	—	1.0	0.8	—	—	—	—
2	100	0	15	100	0	139	1.0	2.2	3.0	1.0	0.8	1.3	—	—	—
3	100	6	78	100	49	117	1.0	4.0	2.2	1.0	0.9	0.8	1.0	0.7	0.1
4	100	7	13	100	0	112	1.0	3.4	4.5	—	—	—	1.0	0.1	0.0
5	100	12	13	—	—	—	1.0	2.1	2.9	—	—	—	1.0	0.4	0.3

Abbreviations: Can, canrenone; PCNA, proliferating cell nuclear antigen; SP, spironolactone.

Each of the five independent skin samples was treated with DMSO, SP, or Can topically or in the media below the biopsy and analyzed for relative XPB protein levels, H2AX phosphorylation, or PCNA protein as described in Figures 1 and 5.

affect DNA metabolism in some way. Given the growing list of cell signaling pathways reported to be targeted by SP (Gabbard et al., 2020), there may be value in better understanding the mechanisms by which high concentrations of these otherwise safe compounds induce toxic effects in skin cells.

MATERIALS AND METHODS

Human skin samples

Human skin experiments utilized skin obtained from discarded skin from panniculectomies and other surgical procedures. Patient consent for experiments was not required because deidentified, leftover surgical human tissue is considered to be discarded material by our institution, and thus the studies were exempt. Small, 8 mm punch biopsies were excised and placed in a 24-well Millicell cell culture insert in a well of a 24-well plate containing 0.5 ml of culture medium (DMEM [Hyclone, Logan, UT] containing 10% fetal bovine serum [Hyclone] and a combination of penicillin and streptomycin [Life Technologies, Grand Island, NY]) (Choi et al., 2020; Kemp et al., 2019). For addition of compounds to the culture medium, 1 μl of DMSO or a 10 mM stock of SP or Can (Sigma-Aldrich) were added to the medium (to obtain a final concentration of 20 μM). For topical treatments, 25 μl of a 120 mM (5%) SP or Can solution (or DMSO vehicle) was pipetted onto the epidermis of the biopsy. Treatments were repeated 24 hours later, and then the biopsies were snap frozen in liquid nitrogen 48 hours after the first treatment. Additional biopsies were fixed in formalin and then embedded in paraffin, sectioned, and stained with H&E by AML Laboratories (St. Augustine, FL). Slides were visualized using a Cytation 5 Imaging Multi-Mode Reader (BioTek, Winooski, VT).

Cell culture

HaCaT cells were grown in DMEM containing 10% fetal bovine serum and penicillin and/or streptomycin. Telomerase-immortalized neonatal KCs were cultured as previously described in EpiLife medium (Life Technologies) containing human KC growth supplement and penicillin and/or streptomycin (Kemp et al., 2019). DMSO, SP, or Can was added to the culture medium at the indicated concentrations. The ATR inhibitor VE-821 and pan-caspase inhibitor Z-VAD-FMK were purchased from Selleckchem (Houston, TX), dissolved in DMSO, and used at 10 μM and 20 μM, respectively. Cell proliferation assays were performed by treating cells in triplicate wells of 96-well plates with the indicated compounds (or vehicle and/or DMSO control) for 2 days. Cells were then incubated with 0.25 mg/ml thiazolyl blue tetrazolium bromide (Sigma-Aldrich) for 1 hour, and the dye solubilized in DMSO was measured by absorbance at 570 nm. Relative survival was quantified by normalizing the absorbance values to the DMSO control and then to the untreated drug control. GraphPad Prism 8 (GraphPad Software, San Diego, CA) was used to perform nonlinear regressions and to calculate half-maximal inhibitory concentration values.

Immunoblotting

To prepare skin epidermal samples for immunoblot analysis, the punch biopsies were briefly heated in a water bath at 60–70 °C for 6 seconds and then placed in an ice bath for 9 seconds. A curette was then used to separate the dermis from the epidermis, which was then sonicated in RIPA buffer and centrifuged for 20 minutes at maximum speed in a microcentrifuge at 4 °C. To prepare protein lysates from cultured KCs, cells were lysed in 20 mM Tris-hydrogen chloride (pH 7.4) (Fisher Bioreagents, Fair Lawn, NJ), 150 mM sodium chloride (Research Products International, Mt. Prospect, IL), 1 mM EDTA (Fisher Bioreagents), 1 mM EGTA (Fisher Bioreagents), and 1% Triton X-100 (Fisher Bioreagents) and centrifuged for 15–20 minutes at maximum speed in a microcentrifuge at 4 °C. The soluble fraction was transferred to a new tube, and the residual, chromatin pellet was sonicated in the same lysis buffer. The soluble or chromatin-enriched fractions were then separated by SDS-PAGE, transferred to a nitrocellulose membrane, and then stained with Ponceau S to ensure equal protein loading. After washing with Tris-buffered saline containing 0.1% Tween-20 (Fisher Bioreagents) and blocking in 5% milk in Tris-buffered saline containing 0.1% Tween-20, blots were probed with dilutions of antibodies against XPB (Santa Cruz sc-293, Santa Cruz Biotechnology, Dallas, TX), actin (Bethyl A300-485A, Bethyl Laboratories, Montgomery, TX), or phosphorylated Chk1 (Ser345; Cell Signaling #2348, Cell Signaling Technology, Danvers, MA); Chk1 (Santa Cruz sc-8408, Santa Cruz Biotechnology), monoubiquitinated PCNA (Cell Signaling #13439, Cell Signaling Technology), or PCNA (Santa Cruz sc-56, Santa Cruz Biotechnology); and phosphorylated Chk2 (Thr68; Cell Signaling #2661, Cell Signaling Technology), phosphorylated p53 (Cell Signaling sc-9248, Cell Signaling Technology), phosphorylated KAP1 (Bethyl A300-767A, Bethyl Laboratories), Caspase 3 (Cell Signaling #9665, Cell Signaling Technology), PARP (Cell Signaling #9542, Cell Signaling Technology), or phosphorylated histone H2AX (Ser139; Cell Signaling #9718, Cell Signaling Technology). After washing, the blots were probed with horseradish peroxidase–coupled anti-rabbit IgG (Thermo Fisher Scientific, Waltham, MA) secondary antibody for 1–2 hours at room temperature. Chemiluminescence was visualized with either Clarity Western ECL substrate (Bio-Rad Laboratories, Hercules, CA) or SuperSignal West Femto substrate (Thermo Scientific Scientific) using a Molecular Imager Chemi-Doc XRS+ imaging system (Bio-Rad Laboratories). Signals in the linear range of detection were quantified by densitometry using Image Lab (Bio-Rad Laboratories) and normalized as previously described (Kemp et al., 2019) or calculated as fold changes relative to those of the DMSO-treated sample. BrdU dot blotting was performed as previously reported (Kemp et al., 2017). GraphPad Prism 8 was used to perform statistical analyses and nonlinear regressions.

Data availability statement

No datasets were generated or analyzed during this study.

ORCIDs

M. Alexandra Carpenter: http://orcid.org/0000-0001-8976-7969
Michael G. Kemp: http://orcid.org/0000-0001-8203-0745

AUTHOR CONTRIBUTIONS

Conceptualization: MGK; Formal Analysis: MAC, MGK; Funding Acquisition: MGK; Investigation: MAC, MGK; Methodology: MAC, MGK; Supervision: MGK; Writing - Original Draft Preparation: MGK; Writing - Review and Editing: MAC, MGK

ACKNOWLEDGMENTS

This work was supported by start-up funding by Wright State University (to MGK) and by a grant from the National Institute of General Medical Sciences (GM130583 to MGK). We thank the Wright State University (Dayton, OH) Proteome Analysis Laboratory for the use of equipment to carry out this work.

CONFLICT OF INTEREST

The authors state no conflict of interest.

Disclaimer

The content of this paper is solely the responsibility of the authors and does not necessarily represent the official views of the National Institutes of Health.

REFERENCES

Abdel-Raouf H, Aly UF, Medhat W, Ahmed SS, Abdel-Aziz RTA. A novel topical combination of minoxidil and spironolactone for androgenetic alopecia: clinical, histopathological, and physicochemical study. Dermatol Ther 2021a;34:e14678.

Alekseev S, Ayadi M, Brino L, Egly JM, Larsen AK, Coin F. A small molecule screen identifies an inhibitor of DNA repair inducing the degradation of TFIIH and the chemosensitization of tumor cells to platinum. Chem Biol 2014;21:398–407.

Andressoo JO, Weeda G, de Wit J, Mitchell JR, Beems RB, van Steeg H, et al. An Xpb mouse model for combined xeroderma pigmentosum and Cockayne syndrome reveals progeroid features upon further attenuation of DNA repair. Mol Cell Biol 2009;29:1276–90.

Arai K, Homma T, Morikawa Y, Ubukata N, Tsuruoka H, Aoki K, et al. Pharmacological profile of CS-3150, a novel, highly potent and selective non-steroidal mineralocorticoid receptor antagonist. Eur J Pharmacol 2015;761:226–34.

Biggar RJ, Andersen EW, Wohlfahrt J, Melbye M. Spironolactone use and the risk of breast and gynecologic cancers. Cancer Epidemiol 2013;37:870–5.

Biyashev D, Onay UV, Dalal P, Demczuk M, Evans S, Techner JM, et al. A novel treatment for skin repair using a combination of spironolactone and vitamin D3. Ann N Y Acad Sci 2020;1480:170–82.

Boix J, Nguyen VT, Farman N, Aractingi S, Pérez P. Mineralocorticoid receptor blockade improves glucocorticoid-induced skin atrophy but partially ameliorates anti-inflammatory actions in an irritative model in human skin explants. Exp Dermatol 2018;27:185–7.

Bonne C, Raynaud JP. Mode of spironolactone anti-androgenic action: inhibition of androstanolone binding to rat prostate androgen receptor. Mol Cell Endocrinol 1974;2:59–67.

Bowman JD, Kim H, Bustamante JJ. Drug-induced gynecomastia. Pharmacotherapy 2012;32:1123–40.

Caballero R, Moreno I, González T, Arias C, Valenzuela C, Delpón E, et al. Spironolactone and its main metabolite, canrenoic acid, block human ether-a-go-go-related gene channels. Circulation 2003;107:889–95.

Chauhan AK, Li P, Sun Y, Wani G, Zhu Q, Wani AA. Spironolactone-induced XPB degradation requires TFIIH integrity and ubiquitin-selective segregase VCP/p97. Cell Cycle 2021;20:81–95.

Choi JH, Han S, Kemp MG. Detection of the small oligonucleotide products of nucleotide excision repair in UVB-irradiated human skin. DNA Repair (Amst) 2020;86:102766.

Compe E, Egly JM. TFIIH: when transcription met DNA repair [published correction appears in Nat Rev Mol Cell Biol 2012;13:476. Nat Rev Mol Cell Biol 2012;13:343–54.

Corvol P, Michaud A, Menard J, Freifeld M, Mahoudeau J. Antiandrogenic effect of spirolactones: mechanism of action. Endocrinology 1975;97:52–8.

Cranston WI, Juel-Jensen BE. The effects of spironolactone and chlorthalidone on arterial pressure. Lancet 1962;1:1161–4.

Dai Y, Grant S. New insights into checkpoint kinase 1 in the DNA damage response signaling network. Clin Cancer Res 2010;16:376–83.

Dojki FK, Bakris G. Nonsteroidal mineralocorticoid antagonists in diabetic kidney disease. Curr Opin Nephrol Hypertens 2017;26:368–74.

Elinoff JM, Chen LY, Dougherty EJ, Awad KS, Wang S, Biancotto A, et al. Spironolactone-induced degradation of the TFIIH core complex XPB subunit suppresses NF-κB and AP-1 signalling. Cardiovasc Res 2018;114:65–76.

Fishburn J, Tomko E, Galburt E, Hahn S. Double-stranded DNA translocase activity of transcription factor TFIIH and the mechanism of RNA polymerase II open complex formation. Proc Natl Acad Sci USA 2015;112:3961–6.

Fuss JO, Tainer JA. XPB and XPD helicases in TFIIH orchestrate DNA duplex opening and damage verification to coordinate repair with transcription and cell cycle via CAK kinase. DNA Repair (Amst) 2011;10:697–713.

Gabbard RD, Hoopes RR, Kemp MG. Spironolactone and XPB: an old drug with a new molecular target. Biomolecules 2020;10:756.

Gardiner P, Schrode K, Quinlan D, Martin BK, Boreham DR, Rogers MS, et al. Spironolactone metabolism: steady-state serum levels of the sulfur-containing metabolites. J Clin Pharmacol 1989;29:342–7.

Gómez R, Núñez L, Caballero R, Vaquero M, Tamargo J, Delpón E. Spironolactone and its main metabolite canrenoic acid block hKv1.5, Kv4.3 and Kv7.1 + minK channels. Br J Pharmacol 2005;146:146–61.

Goodarzi AA, Noon AT, Deckbar D, Ziv Y, Shiloh Y, Löbrich M, et al. ATM signaling facilitates repair of DNA double-strand breaks associated with heterochromatin. Mol Cell 2008;31:167–77.

Ilic D, Cvetkovic M, Tasic-Kostov M. Emulsions with alkyl polyglucosides as carriers for off-label topical spironolactone - safety and stability evaluation. Pharm Dev Technol 2021;26:373–9.

Kagawa CM, Cella JA, Van Arman CG. Action of new steroids in blocking effects of aldosterone and desoxycorticosterone on salt. Science 1957;126:1015–6.

Kanao R, Masutani C. Regulation of DNA damage tolerance in mammalian cells by post-translational modifications of PCNA. Mutat Res 2017;803–805:82–8.

Kelidari HR, Saeedi M, Akbari J, Morteza-Semnani K, Gill P, Valizadeh H, et al. Formulation optimization and in vitro skin penetration of spironolactone loaded solid lipid nanoparticles. Colloids Surf B Biointerfaces 2015;128:473–9.

Kelidari HR, Saeedi M, Akbari J, Morteza-Semnani K, Valizadeh H, Maniruzzaman M, et al. Development and optimisation of spironolactone nanoparticles for enhanced dissolution rates and stability. AAPS PharmSciTech 2017;18:1469–74.

Kelidari HR, Saeedi M, Hajheydari Z, Akbari J, Morteza-Semnani K, Akhtari J, et al. Spironolactone loaded nanostructured lipid carrier gel for effective treatment of mild and moderate acne vulgaris: a randomized, double-blind, prospective trial. Colloids Surf B Biointerfaces 2016;146:47–53.

Kemp MG, Krishnamurthy S, Kent MN, Schumacher DL, Sharma P, Excoffon KJDA, et al. Spironolactone depletes the XPB protein and inhibits DNA damage responses in UVB-irradiated human skin. J Invest Dermatol 2019;139:448–54.

Kemp MG, Spandau DF, Simman R, Travers JB. Insulin-like growth factor 1 receptor signaling is required for optimal ATR-CHK1 kinase signaling in ultraviolet B (UVB)-irradiated human keratinocytes. J Biol Chem 2017;292:1231–9.

Kitagawa R, Kastan MB. The ATM-dependent DNA damage signaling pathway. Cold Spring Harb Symp Quant Biol 2005;70:99–109.

Lacombe B, Morel M, Margottin-Goguet F, Ramirez BC. Specific inhibition of HIV infection by the action of spironolactone in T cells. J Virol 2016;90:10972–80.

Leung WH, Vong QP, Lin W, Janke L, Chen T, Leung W. Modulation of NKG2D ligand expression and metastasis in tumors by spironolactone via RXRgamma activation. J Exp Med 2013;210:2675–92.

Liddle GW. Sodium diuresis induced by steroidal antagonists of aldosterone. Science 1957;126:1016–8.

Mackenzie IS, Morant SV, Wei L, Thompson AM, MacDonald TM. Spironolactone use and risk of incident cancers: a retrospective, matched cohort study. Br J Clin Pharmacol 2017;83:653–63.

Martella C, Tollenaere AI, Waast L, Lacombe B, Groussaud D, Margottin-Goguet F, et al. Human T-cell lymphotropic virus type 1 transactivator tax exploits the XPB subunit of TFIIH during viral transcription. J Virol 2020;94.e02171–19.

Maubec E, Laouénan C, Deschamps L, Nguyen VT, Scheer-Senyarich I, Wackenheim-Jacobs AC, et al. Topical mineralocorticoid receptor blockade limits glucocorticoid-induced epidermal atrophy in human skin. J Invest Dermatol 2015;135:1781–9.

Moore KP, Aithal GP. Guidelines on the management of ascites in cirrhosis. Gut 2006;55(Suppl. 6):vi1–12.

Mukherjee B, Kessinger C, Kobayashi J, Chen BPC, Chen DJ, Chatterjee A, et al. DNA-PK phosphorylates histone H2AX during apoptotic DNA fragmentation in mammalian cells. DNA Repair (Amst) 2006;5:575–90.

Nguyen VT, Farman N, Maubec E, Nassar D, Desposito D, Waeckel L, et al. Re-epithelialization of pathological cutaneous wounds is improved by local mineralocorticoid receptor antagonism. J Invest Dermatol 2016;136:2080–9.

Park H, Skopit S. Safety considerations and monitoring in patients treated with systemic medications for acne. Dermatol Clin 2016;34:185–93.

Rathnayake D, Sinclair R. Use of spironolactone in dermatology. Skinmed 2010;8:328–32. quiz 333.

Salama A, Badran M, Elmowafy M, Soliman GM. Spironolactone-loaded LeciPlexes as potential topical delivery systems for female acne: in vitro appraisal and ex vivo skin permeability studies. Pharmaceutics 2019;12:25.

Saldivar JC, Cortez D, Cimprich KA. The essential kinase ATR: ensuring faithful duplication of a challenging genome [published correction appears in Nat Rev Mol Cell Biol 2017;18:783]. Nat Rev Mol Cell Biol 2017;18:622–36.

Shahar OD, Kalousi A, Eini L, Fisher B, Weiss A, Darr J, et al. A high-throughput chemical screen with FDA approved drugs reveals that the antihypertensive drug spironolactone impairs cancer cell survival by inhibiting homology directed repair. Nucleic Acids Res 2014;42:5689–701.

Sinclair R, Patel M, Dawson TL Jr, Yazdabadi A, Yip L, Perez A, et al. Hair loss in women: medical and cosmetic approaches to increase scalp hair fullness. Br J Dermatol 2011;165(Suppl. 3):12–8.

Solier S, Pommier Y. The apoptotic ring: a novel entity with phosphorylated histones H2AX and H2B and activated DNA damage response kinases. Cell Cycle 2009;8:1853–9.

Sønder SU, Woetmann A, Odum N, Bendtzen K. Spironolactone induces apoptosis and inhibits NF-kappaB independent of the mineralocorticoid receptor. Apoptosis 2006;11(12):2159–65.

Sturtevant FM. Antihypertensive effects of an aldosterone antagonist. Science 1958;127:1393–4.

Szalat R, Samur MK, Fulciniti M, Lopez M, Nanjappa P, Cleynen A, et al. Nucleotide excision repair is a potential therapeutic target in multiple myeloma. Leukemia 2018;32:111–9.

Ueda M, Matsuura K, Kawai H, Wakasugi M, Matsunaga T. Spironolactone-induced XPB degradation depends on CDK7 kinase and SCF^{FBXL18} E3 ligase. Genes Cells 2019;24:284–96.

Verma D, Thompson J, Swaminathan S. Spironolactone blocks Epstein-Barr virus production by inhibiting EBV SM protein function. Proc Natl Acad Sci USA 2016;113:3609–14.